ISBN: 978-3-95450-132-8 doi:10.18429/JACoW-IPAC2014-WEPME064

COMPARISON OF AN ANALYTICAL MODEL FOR LOSSY TRANSMISSION LINES WITH MEASURMENT DATA.*

N. Schmitt, H. Klingbeil, GSI, Darmstadt, Germany†

Abstract

This paper deals with the analytical modeling of lossy coaxial transmission lines in the frequency range from 100 kHz to 50 MHz with focus on corrugated coaxial lines with polyethylene foam as dielectric. The considered transmission lines are used in low-level radio frequency (LLRF) systems (< 5 MHz) at GSI. These applications require a high precision in amplitude and phase for the transmitted signals where a detailed knowledge of the line properties is of significant interest. As the corresponding data sheets do not provide appropriate data, the necessary data have been computed. The obtained results from the purely analytical model were then compared with previous measurements for validation purposes.

INTRODUCTION

Various applications at the GSI Helmholtzzentrum für Schwerionenforschung GmbH require low-level radio frequency (LLRF) systems. Due to a low relativistic beta at the beginning of a machine cycle for the heavy ion synchrotron (SIS 18) and small harmonic numbers, frequencies down to hundreds of kHz are used to generate the gap voltage and occur as measurement signals, e.g. at the beam pick up. Especially the latter have to be transmitted over long distances in a range of $50 - 150$ m from the accelerator tunnel to a bunker where sensitive signal processing electronics are sufficiently protected against radiation. This principle is briefly illustrated in Figure 2. The transmission of these low voltage signals ($0 - 10$ V) requires high noise immunity in order to maintain amplitude and phase information. Also high attenuation must be avoided. Otherwise, unacceptable errors for the further usage of the amplified signal (e.g. feedback systems) could occur. Those systems require a measurement signal with a precision of less than 1% relative error in phase and amplitude. We would like to point out that the wavelength at which the mismatching to the 50 Ω system appears is in the range of hundreds of m and might give reasons to assume that wave propagation effects are not dominating anymore. This however is not the case because the used line lengths exceed the common laboratory sizes. Most manufacturers of coaxial lines do not provide appropriate data in the required frequency range. Therefore, this work applies an analytical broadband model for three coaxial transmission lines, namely LDF1RK-50 (LDF), FSJRK-50B (FSJ), and LCF12-50JFN (LCF). The model proposed by [1] and used in [4] combines analytical electrostatic and radio frequency (RF) line parameters in order to build a bridge from the DC to the AC domain.

* Work supported by GSI and TU-Darmstadt
† klingbeil@temf.tu-darmstadt.de

Figure 1: The transmission line is manufactured of a round inner conductor which is separated from the corrugated outer conductor by a polyethylene (PE) foam as dielectric and surrounded by an isolating layer.

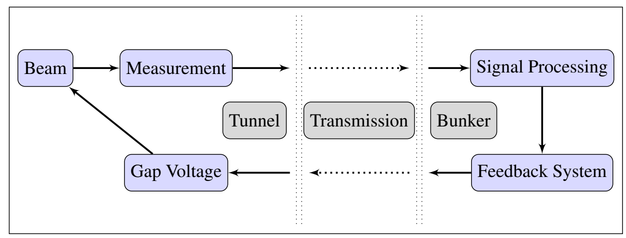

Figure 2: Information flow chart of the SIS 18. After measuring the beam, the signal is transmitted from the accelerator tunnel to the bunker where sensitive electronics are located. The processed data reacts to the beam by means of phase or amplitude manipulation of the RF-Voltage.

ANALYTICAL MODEL

We will now briefly present the mentioned model for the analytical modeling of lossy coaxial transmission lines as proposed by [1]. Figure 3 illustrates the used transmission

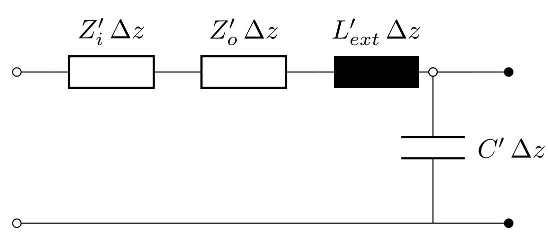

Figure 3: Extended schematic representation of the elemenary components of a coaxial transmission line [1]. Z_i' and Z_o' denote the per-length impedances of the inner and outer conductor. L_{ext}' and C' are the external per-length inductance and capacitance, respectively.

line model. The resulting characteristic impedance and the latter mentioned quantities are given by:

$$Z_L(\omega) = \sqrt{\frac{Z'(\omega)}{Y'(\omega)}} = R_L + iX_L, \tag{1}$$

ISBN: 978-3-95450-132-8 doi:10.18429/JACoW-IPAC2014-WEPME064

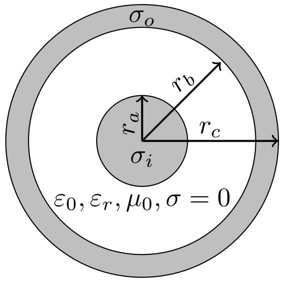

Figure 4: Cross section of a lossy coaxial transmission line. The radii r_a, r_b, r_c are constant as well as the relative permittivity ε_r and the outer and inner conductivity σ_o and σ_i.

where

$$\begin{aligned} Z'(\omega) &= i\omega L'_{ext} + Z'_i(\omega) + Z'_o(\omega) \\ &=: R' + i\omega L', \end{aligned} \tag{2}$$

$$Y'(\omega) = i\omega C', \tag{3}$$

and

$$Z'_t(\omega) = R'_{t,\mathrm{DC}} + \frac{i\omega L'_{t,int}\left(R'_{t,\mathrm{RF}}(\omega) + i\omega L'_{t,\mathrm{RF}}(\omega)\right)}{R'_{t,\mathrm{RF}}(\omega) + i\omega\left(L'_{t,\mathrm{RF}}(\omega) + L'_{t,int}\right)}. \tag{4}$$

Here, $t \in \{i, o\}$ denotes the inner or outer conductor. The per-length quantities $R'_{t,\mathrm{DC}}, R'_{t,\mathrm{RF}}, L'_{t,int}, L'_{t,RF}$, and C' can be obtained from field theory and are also listed in [1]. A sketch of the line cross section is shown in Figure 4. For the purpose of comparison between the analytically obtained line characteristics with the measurement results, R_L and X_L according to (1) will be taken as the main figure of merit.

LINE GEOMETRY DIFFICULTIES

The previously presented model shows high consistency with the exact analytical Schelkunoff [2] formulas and the measurement results for non corrugated transmission lines according to recent measurements at GSI. Unfortunately this is no longer the case for the corrugated lines considered here. One of the main problems is the definition of the radii r_b and r_c since those vary periodically in propagation direction as shown Figure 1 and 5.

In order to include the corrugation, we propose to average the line parameters over one corrugation period. Modeling the corrugation pattern sinusoidally with a constant thickness of the outer conductor, the radius r_b reads

$$r_b(z) := r_b + \Delta_o \sin\left(\frac{2\pi}{\Delta z}\, z\right), \quad z \in [0, \Delta z], \tag{5}$$

where r_b is the mean of the outer radius and Δ_o the corrugation amplitude. Inserting this definition of the outer

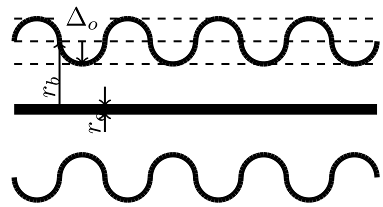

Figure 5: Cross section along the propagation direction of the corrugated transmission line. Since the outer conductor is not translation invariant, the geometric interpretation of the outer radii varies with respect to the position.

radius and averaging over one period leads to

$$R'_{o,\mathrm{RF}} = \frac{1}{\Delta z}\int_0^{\Delta z} \frac{1}{2\pi r_b(z)}\mathrm{d}z \sqrt{\frac{\omega\mu_0}{2\sigma_o}}, \tag{6}$$

$$L'_{o,\mathrm{RF}} = \frac{1}{\Delta z}\int_0^{\Delta z} \frac{1}{2\pi r_b(z)}\mathrm{d}z \sqrt{\frac{\mu_0}{2\sigma_o\omega}}, \tag{7}$$

$$\begin{aligned} L'_{o,int} = \frac{1}{\Delta z}\int_0^{\Delta z} & \frac{(r_b(z)+\Delta_c)^4 \ln\left(\frac{r_b(z)+\Delta_c}{r_b(z)}\right)}{\left((r_b(z)+\Delta_c)^2 - r_b(z)^2\right)^2} \\ & + \frac{r_b(z)^2 - 3\left(r_b(z)+\Delta_c\right)^2}{4\left((r_b(z)+\Delta_c)^2 - r_b(z)^2\right)}\mathrm{d}z \cdot \frac{\mu_0}{2\pi}, \end{aligned} \tag{8}$$

and

$$C' = \frac{1}{\Delta z}\int_0^{\Delta z} \frac{2\pi\varepsilon_0\varepsilon_r}{\ln\left(\frac{r_b(z)}{r_a}\right)}\mathrm{d}z. \tag{9}$$

Here, ε_r is the relative permeability and Δ_c the thickness of the outer conductor. It may be pointed out that (6), (7), (8), and (9) do not use an average over the radius but an average over the per-length quantities itself. We have only modified the formulas for quantities where the outer radius occurs while the remaining ones stay as given in [1].

COMPARISON WITH MEASUREMENT

Using measurement data from GSI, we now want to verify the model described above in a frequency regime of $f_{min} = 200$ kHz up to $f_{max} = 50$ MHz. Although the upper limit is far beyond the desired frequency range it is important to see a convergence of the model to the data sheet value given for frequencies above 5 MHz.

The measurements were performed with an Agilent Vector Network Analyzer (VNA), model 87553ES [3] that was calibrated using the type N calibration kit. Through a one-port measurement, the S_{11} reflection coefficient was measured in a short- and open-circuit configuration in order to obtain the input impedance of each setup. Table 1 shows the measurement error. Evaluating (1) together with the modifications proposed in the previous section and using

ISBN: 978-3-95450-132-8 doi:10.18429/JACoW-IPAC2014-WEPME064

Table 1: Typical maximum deviation of the measured characteristic impedance Z_{L}. The considered frequency range is 200 kHz to 4 MHz

	$\Delta\mathrm{Re}\{Z_{\mathrm{L}}\}$ (%)	$\Delta\mathrm{Im}\{Z_{\mathrm{L}}\}$ (%)
LDF	2	7
LCF	2	10
FSJ	2	4

Table 2: Typical data sheet values of the lines LDF , FSJ , and LCF , with polyethylene (PE) foam as dielectric.

	LDF	FSJ	LCF
ε_r	1.35	1.42	1.29
r_a: Outer Radius Inner Cond. (mm)	1.27	0.95	2.4
r_b: Outer Radius Dielectric (mm)	3.07	2.41	5.95
Δ_o: Corrugation Amplitude Outer Cond. (mm)	0.36	0.35	0.5
Δ_c: Thickness Outer Cond. (mm)	0.4	0.2	0.4
Material Inner Cond.	Copper-clad aluminium, solid		
Material Outer Cond.	Corrugated copper, solid		
Inner Cond. $R'_{i,\mathrm{DC}}$ (Ω/km)	5.2	9.8	1.6
Outer Cond. $R'_{o,\mathrm{DC}}$ (Ω/km)	4	6.6	2.7

the values given in Table 2 produces the plots in Figure 6 and Figure 7 for R_L and X_L, respectively. While the modeling of the real part works very well, it shows larger errors for the imaginary part. For LCF we could obtain the best results whereas the modeled curves for FSJ and LDF leave the vicinity of the measurement error for frequencies below 1 MHz. This result might be mainly driven by the smaller diameter of LDF and FSJ and higher influence of the actual corrugation pattern which we assumed to be sinusoidal.

CONCLUSION

In this work, the analytical modeling of corrugated coaxial transmission lines in the lower MHz was presented and then compared with the measurement data. The model achieved an agreement of better than 3% for the real part of the characteristic impedance whereas it led to much larger errors for the imaginary part. The results will be used to optimize the LLRF systems of GSI's SIS-18 with respect to phase and amplitude accuracies.

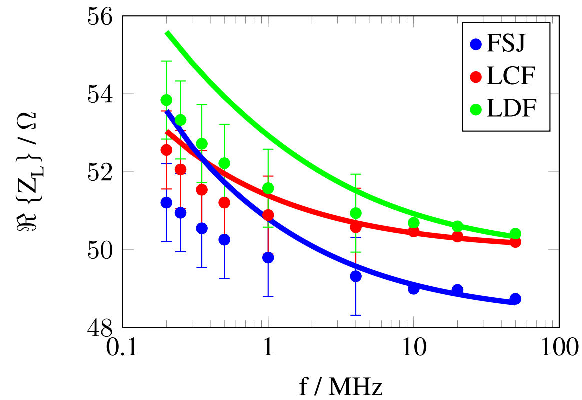

Figure 6: Real part of the characteristic impedance Z_L. The continuous graphs represent the values computed with (1) while the dots show the corresponding measurement points.

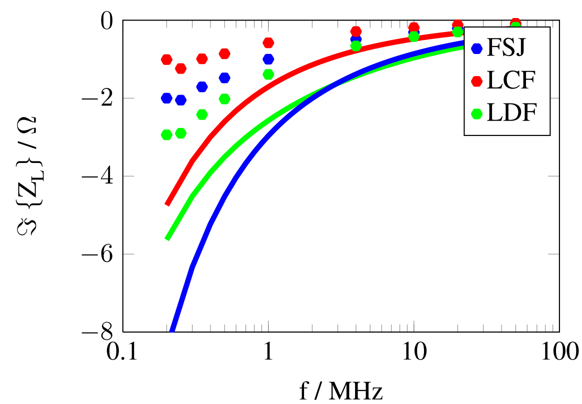

Figure 7: Imaginary part of the characteristic impedance Z_L. Same setup as in Figure 6, but deviation between measurement and model is much higher (ordinate scale). Here, the error bars are comparably small and thus left out. The errors are given in Table 1.

ACKNOWLEDGMENT

This work was supported by GSI and TU Darmstadt. I would like to give many thanks to the Joint Universities Accelerator School (JUAS) which granted my participation at the International Particle Accelerator Conference 2014 enabling me to present these results.

REFERENCES

[1] F. M. Tesche, IEEE Trans. Electromagn. Compat. **49**, 12 (2007).

[2] S. A. Schelkunoff, Bell Syst. Tech, J. **13**(4), 532 (1934).

[3] Agilent Technologies, Agilent Network Analyzer Basics (5965-7917E).

[4] D. E. Charrier et al., Measuring and modeling line parameters of lossy coaxial transmission lines at low operating frequencies (submitted to 'Electrical Engineering').